MedChemComm

RSC Publishing

CONCISE ARTICLE

Development of a diketopiperazine-forming dipeptidyl Gly-Pro spacer for preparation of an antibody–drug conjugate†

Cite this: *Med. Chem. Commun.*, 2013, **4**, 792

Received 5th March 2013
Accepted 5th March 2013

DOI: 10.1039/c3md00075c

www.rsc.org/medchemcomm

Shino Manabe,*[a] Hikaru Machida,[b] Yoshiyuki Aihara,[a] Masahiro Yasunaga,[b] Yukishige Ito[a] and Yasuhiro Matsumura*[b]

We developed a novel diketopiperazine-forming dipeptidyl spacer aimed at application in antibody–drug conjugates. Enzymatic cleavage of a peptide linked to the Gly-Pro spacer resulted in formation of diketopiperazine, which was stable and non-toxic, and release of the parent drug.

Introduction

Antibody–drug conjugates (ADCs) play an increasingly important role in selective delivery of potent drugs to their intended site of action in the body.[1–3] There is a strong demand for efficient ADC molecule design, especially for cancer chemotherapy, because most chemotherapeutic medicines have a narrow safety margin, resulting in severe adverse effects. Recently, several ADCs have been developed, some of which have appeared promising in clinical trials.[4,5] An ADC consists of 3 components: a monoclonal antibody that targets a tumor antigen, a cytotoxic agent, and a linker (Fig. 1). The antibody is a pilot molecule for delivery of an anti-cancer agent. The linker is further divided into a specifier and a spacer. The linker moiety is located between the parent drug and the antibody and increases the rate of enzymatic cleavage. The specifier serves as a substrate for an enzyme with site-specific activity. In the absence of a spacer, enzymatic cleavage of the bond between the specifier and the parent drug may sometimes be inadequate, because of steric hindrance caused by the parent drug.[6,7] Once the bond between the carrier and the linker is cleaved, the spacer should spontaneously release the drug in its active form. In our development of ADCs,[8–10] we focused on a novel linker development.

The most widely used spacer is a *p*-aminobenzyloxycarbonyl spacer.[11] Once the amide bond between the specifier and the spacer has been cleaved, the spacer degrades in a self-immolative manner, and the parent drug is released. During degradation, a highly reactive iminoquinone methide intermediate is formed, which may interact with cellular nucleophiles, such as glutathione, a thiol (Scheme 1).[12] Some endopeptidases, such as prostate-specific antigen, only cleave the amide bonds between amino acids; therefore, the carbamate site in the *p*-aminobenzyloxycarbonyl spacer is sometimes not cleaved by endopeptidases.[13–15]

In this study, we designed a novel spacer for use in a versatile ADC strategy. The spacer consists of a proline-glycine (Gly-Pro) dipeptide, and easily formed diketopiperazine by cyclization. The rate of diketopiperazine formation depends on the proportion of *cis*/*trans* amide isomers of the dipeptide. Although most peptide sequences adopt only the energetically favorable *trans* conformation, proline is unique in that it has a *cis*-amide conformation.[16,17] Thus, proline greatly enhances the rate of diketopiperazine formation because of its great propensity to adopt the *cis*-amide conformation.

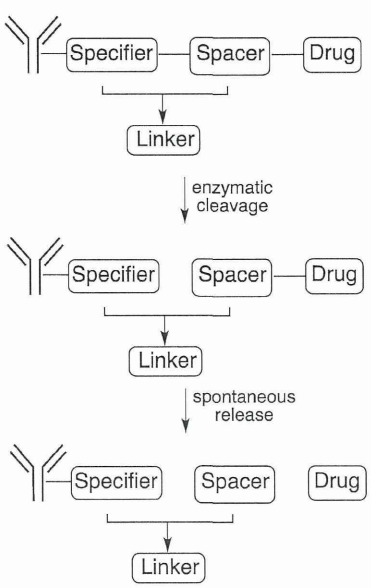

Fig. 1 Components of antibody–drug conjugates.

[a]*RIKEN, Advanced Science Institute, Synthetic Cellular Chemistry Laboratory, Hirosawa, Wako, Saitama 351-0198, Japan. E-mail: smanabe@riken.jp; Fax: +81 48 462 4680; Tel: +81 48 467 9432*

[b]*Investigative Treatment Division, Research Center for Innovative Oncology, National Cancer Center Hospital East, Kashiwa, Chiba 277-0882, Japan. E-mail: yhmatsum@east.ncc.go.jp; Fax: +81 4713 6857; Tel: +81 4713 6857*

† Electronic supplementary information (ESI) available: Experimental details and ^{1}H-NMR and ^{13}C-NMR spectra. See DOI: 10.1039/c3md00075c

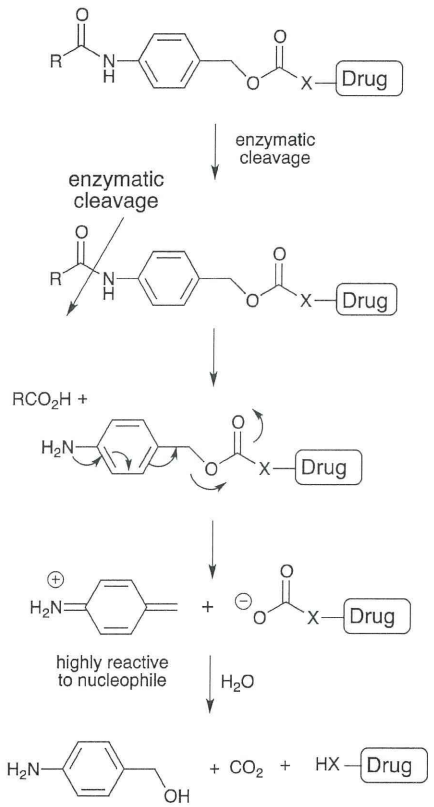

Scheme 1 The *p*-aminobenzyloxycarbonyl spacer degradation mechanism and formation of a highly reactive intermediate; X = NH or O.

In order to minimize the steric hindrance at the enzymatic cleavage site, Gly was chosen for the amino acid site near the cleavage site. The Gly-Pro sequence is well known as a "difficult sequence" for diketopiperazine formation during peptide synthesis.[18–22] Once an enzyme cleaves the peptide bond, the Gly-Pro sequence forms diketopiperazine to release the parent drug in its active form.[23] The diketopiperazine thus formed is normally stable and non-toxic (Scheme 2).

Using this novel spacer, we designed a plasmin-cleavable prodrug for chemotherapy. Plasmin, a serine protease, plays an important role in tumor invasion and metastasis.[24,25] The proteolytically active form of plasmin may be localized around the tumor tissue because it is formed from the inactive proenzyme plasminogen by the urokinase-type plasminogen activator produced by cancer and/or stroma cells.[7,26–30] Plasmin activity is very rapidly inhibited by inhibitors, such as α_2-anti-plasmin, present within the blood circulation. Thus, plasmin is a very promising enzyme for use in a tumor-specific prodrug approach. Since the recognition sequence for cleavage by plasmin is a Val-Leu-Lys tripeptide, we synthesized paclitaxel–peptide conjugates **1** and **2** (Fig. 2). These compounds have a Gly-Pro spacer-containing pentapeptide; unnatural (D)-proline was used for the linker in compound **2** in order to investigate the influence of stereochemistry on drug-release activity. In order to compare the efficacy of the novel linker, we synthesized compound **3**, containing the commonly used *p*-aminobenzyloxycarbonyl spacer, and compound **4**, without a spacer. We chose paclitaxel as the parent drug because it is one of the most useful anti-cancer agents clinically. The linker was attached to the 2-hydroxy group, because it is expected to decrease cytotoxic activity by modification of the 2-hydroxy functionality.[31–37] For an initial evaluation of linkers, an acetyl group was chosen for the N-terminus of paclitaxel-conjugated peptides, instead of using maleimide or bromoacetamide for immobilization to the antibody, in order to avoid the instability of maleimide or bromoacetamide during evaluation of drug-release.

Since paclitaxel is sensitive to both acidic and basic conditions, the methoxytrityl (Mmt) group, which is an acid-labile amino-protecting group,[38] was chosen for protecting the side-chain amino group of lysine. The synthesis was achieved as shown in Scheme 3. The sequential synthesis of a pentapeptide

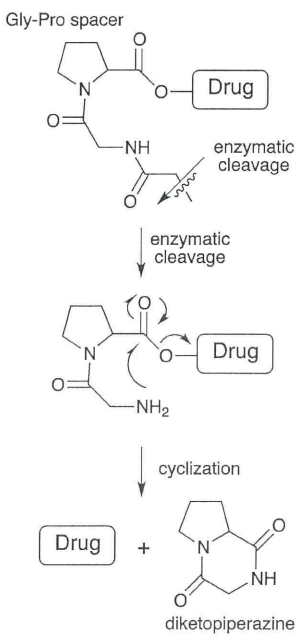

Scheme 2 Drug-release mechanism of the Gly-Pro spacer.

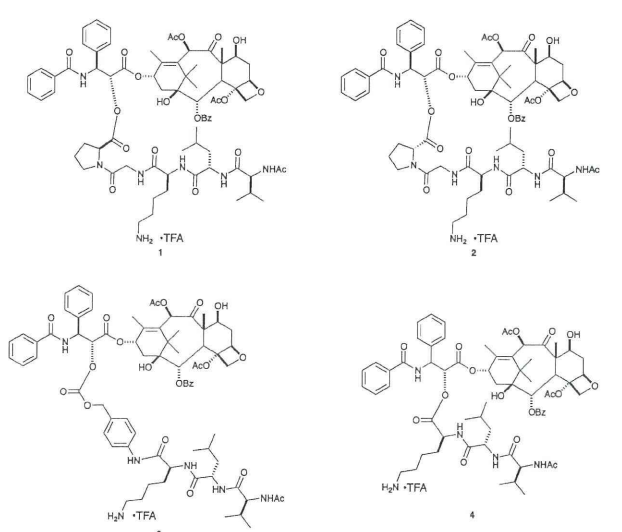

Fig. 2 Synthesized peptide–paclitaxel conjugates.

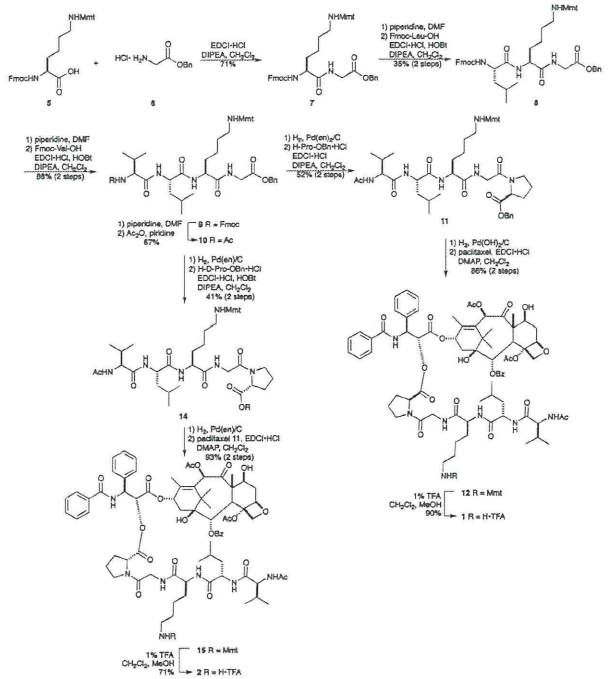

Scheme 3 Synthesis of compounds **1** and **2**.

from C-termini was difficult because of diketopiperazine formation at the dipeptide Fmoc-Gly-Pro-OBn-deprotection step. The pentapeptide is divided into 2 parts, the tetrapeptide and the proline. The Ac-Val-Leu-Lys(Mmt)-Gly-Pro-OBn sequence **10** was prepared in accordance with the Fmoc peptide synthesis strategy. After removal of the benzyl ester[39] of tetrapeptide **10**, (L)-proline was added to the C-terminus. Again, after the hydrogenolysis of the benzyl ester of pentapeptide **11**, the pentapeptide was attached to paclitaxel by water-soluble carbodiimide·hydrochloride (WSCDI·HCl) in the presence of 4-(dimethylamino)pyridine (DMAP). Finally, the Mmt group was removed without intact paclitaxel. The paclitaxel–peptide conjugate **1** was obtained in 71%. Unnatural (D)-proline-containing paclitaxel–peptide was prepared in a similar manner with a 27% overall yield from tetrapeptide **10**.

The less nucleophilic aminobenzyl alcohol **16** was introduced using 2-ethoxy-1-ethoxycarbonyl-1,2-dihydroquinone (EEDQ); then, the peptide was prepared from the C-termini in a sequential manner (Scheme 4). After activation of the hydroxyl

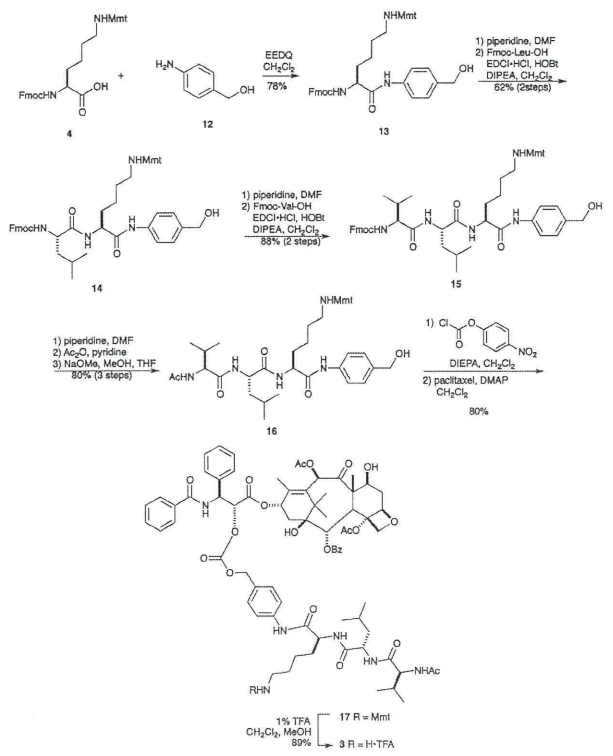

Scheme 4 Synthesis of *p*-aminobenzyloxy spacer-containing paclitaxel–peptide conjugate.

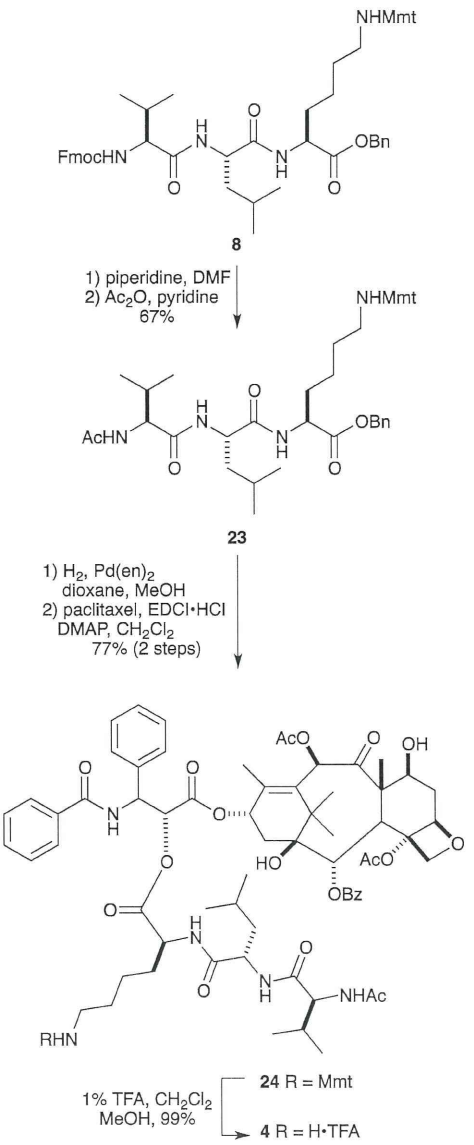

Scheme 5 Synthesis of paclitaxel–tripeptide conjugate **4**.

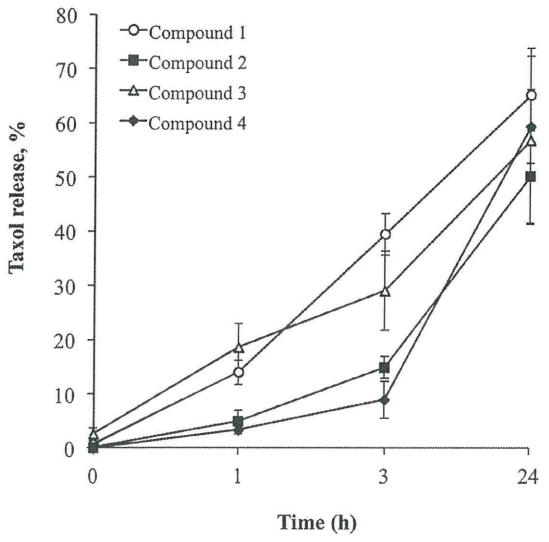

Fig. 3 Paclitaxel releasing ability of compounds **1–4** in the presence of plasmin.

group of the peptide by *p*-nitrophenylcarbonate, the peptide was introduced at the 2-position of paclitaxel.

The tripeptide Ac-Val-Leu-Lys(Mmt)-OH **24** was conjugated to paclitaxel without a linker, with high yield to synthesize compound **4** as shown in Scheme 5.

We next evaluated the ability of linkers to release the paclitaxel in the presence of plasmin (Fig. 3 and Table S1 in the ESI†). As expected, linker-conjugated paclitaxel **1–3** was cleaved in the presence of plasmin within 24 h. The Gly-Pro linker had almost the same efficacy as the compound *p*-aminobenzyloxycarbonyl spacer. Indeed, 39% of paclitaxel was released from compound **1** after 3 h. The unnatural (D)-proline-containing compound **2** was also cleaved by plasmin, although the cleavage rate was slower (15% after 3 h). The tripeptide-conjugated paclitaxel **4** was also cleaved, but the release rate was only 9%. After 24 h, half of the paclitaxel was released from compounds **1–3**.

Conclusions

In conclusion, we designed a novel dipeptidyl spacer to be used as a versatile ADC strategy. The spacer could be easily prepared using well-established peptide chemistry methods. The rate of diketopiperazine formation could be attenuated by choosing the appropriate peptide sequence. This strategy would be applicable to endopeptidases, which only recognize peptide bonds at particular cleavage sites. A detailed study related to the biological activity and pharmacokinetic profile will be reported in future.

Acknowledgements

We thank the Funding Program for World-Leading Innovative R&D on Science and Technology (FIRST Program), Third Term Comprehensive Control Research for Cancer from the Ministry of Health, Labor, and Welfare of Japan, and the National Cancer Center for Promotion of Cancer Research. We thank Ms A. Takahashi for her technical assistance. We are also grateful to Dr S. Daikoku in Glycotrilogy ERATO Project for assistance with the MS measurement and to Professor Hironobu Hojo at Tokai University for discussions.

References

1 S. Jaracz, J. Chen, L. V. Kuznetsova and I. Ojima, *Bioorg. Med. Chem.*, 2005, **13**, 5043.
2 R. V. J. Chari, *Acc. Chem. Res.*, 2008, **41**, 98.
3 S. C. Alley, N. M. Okeley and P. D. Senter, *Curr. Opin. Chem. Biol.*, 2010, **14**, 529.
4 A. Younes, N. L. Bartlett, J. P. Leonard, D. A. Kennedy, C. M. Lynch, E. L. Sievers and A. Forero-Torres, *N. Engl. J. Med.*, 2010, **363**, 1812.
5 S. Verma, D. Miles, L. Gianni, I. E. Krop, M. Welslau, J. Baselga, M. Pegram, D.-Y. Oh, V. Diéras, E. Guardino, L. Fang, M. W. Lu, S. Olsen and K. Blackwell, *N. Engl. J. Med.*, 2012, **367**, 1783.
6 P. K. Chakravarty, P. L. Carl, M. J. Weber and J. A. Katzenellenbogen, *J. Med. Chem.*, 1983, **26**, 638.
7 F. M. de Groot, A. C. de Bart, J. H. Verheijen and H. W. Scheeren, *J. Med. Chem.*, 1999, **42**, 5277.
8 M. Yasunaga, S. Manabe, D. Tarin and Y. Matsumura, *Bioconjugate Chem.*, 2011, **22**, 1776.
9 M. Yasunaga, S. Manabe and Y. Matsumura, *Cancer Sci.*, 2011, **102**, 1396.
10 M. Yasunaga, S. Manabe and Y. Matsumura, *Cancer Sci.*, 2013, **104**, 231.
11 P. L. Carl, P. K. Chakravarty and J. A. Katzenellenbogen, *J. Med. Chem.*, 1981, **24**, 479.
12 During the review process of ref. 11, the same point was made by reviewers. See ref. 13 in ref. 11.
13 S. R. Denmeade, A. Nagy, J. Gao, H. Lilja, A. V. Schally and J. T. Isaacs, *Cancer Res.*, 1998, **58**, 2537.
14 D. DeFeo-Jones, V. M. Garsky, B. K. Wong, D.-M. Feng, T. Bolyar, K. Haskell, D. M. Kiefer, K. Leander, E. McAvoy, P. Lumma, J. Wai, E. T. Senderak, S. L. Motzel, K. Keenan, M. Van Zwieten, J. H. Lin, R. Friedinger, J. Huff, A. Oliff and R. E. Jones, *Nat. Med.*, 2000, **6**, 1248.
15 S. R. Denmeade, C. M. Jakobsen, S. Janssen, S. R. Khan, E. S. Garrett, H. Lilja, S. B. Christensen and J. T. Isaccs, *J. Natl. Cancer Inst.*, 2003, **95**, 990.
16 G. N. Ramachandran and A. K. Mitra, *J. Mol. Biol.*, 1976, **107**, 85.
17 D. E. Stewart, A. Sarkar and J. E. Wampler, *J. Mol. Biol.*, 1990, **214**, 253.
18 B. F. Gisin and R. B. Merrifield, *J. Am. Chem. Soc.*, 1972, **94**, 3102.
19 M. C. Khosla, R. R. Smeby and F. M. Bumpus, *J. Am. Chem. Soc.*, 1972, **94**, 4721.
20 M. Roth and J. Mazanek, *Liebigs Ann. Chem.*, 1974, 439.
21 E. Pedroso, A. Grandas, X. de las Heras, R. Eritja and E. Giralt, *Tetrahedron Lett.*, 1986, **27**, 743.
22 A. Ishidro-Llobet, J. Guasch-Camell, M. Álvarez and F. Albericio, *Eur. J. Org. Chem.*, 2005, 3031 and references therein.
23 The reduction of compound **25** was released paclitaxel, and formation of diketopiperazine was confirmed.

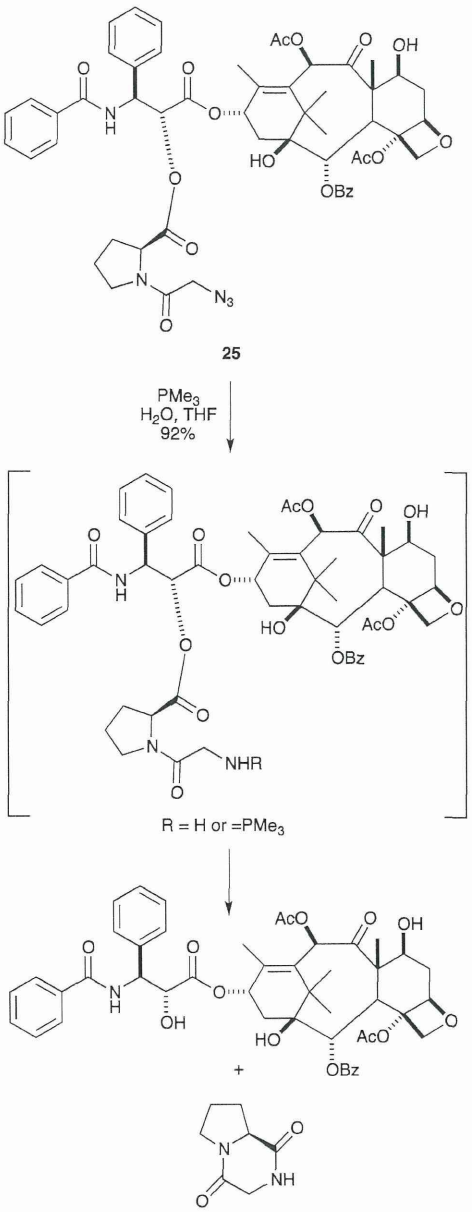

24 S. F. Brady, N. M. Pawluczyk, P. K. Lumma, D.-M. Feng, J. M. Wai, R. Jones, D. DeFeo-Jones, B. K. Wong, C. Miller-Stein, J. H. Lin, A. Oliff, R. M. Freidinger and V. M. Garsky, *J. Med. Chem.*, 2002, **45**, 4706.

25 G. A. R. Y. Suaifan, M. F. Mahon, T. Arafat and M. D. Threadgill, *Tetrahedron*, 2006, **62**, 11245.

26 P. L. Carl, P. K. Chakravarty, J. A. Katzenellenbogen and M. J. Webwe, *Proc. Natl. Acad. Sci. U. S. A.*, 1980, **77**, 2224.

27 G. Eisenbrand, S. Lauck-Birkel and W. C. Tang, *Synthesis*, 1996, 1246.

28 R. Hewitt and K. Dano, *Enzyme Protein*, 1996, **49**, 163.

29 Y.-I. Yamashita and M. Ogawa, *Int. J. Oncol.*, 1997, **10**, 807.

30 U. Ruening, V. Magdolen, O. Wilhelm, K. Fischer, V. Lutz, H. Graeff and M. Schmitt, *Int. J. Oncol.*, 1998, **13**, 893.

31 W. Mellado, N. F. Magri, D. G. I. Kingston, R. Garcia-Arenas, G. A. Orr and S. B. Horwitz, *Biochem. Biophys. Res. Commun.*, 1984, **124**, 329.

32 N. F. Magri and D. G. I. Kingston, *J. Nat. Prod.*, 1988, **51**, 298.

33 J. Kant, S. Huang, H. Wong, C. Fairchild, D. Vyas and V. Farina, *Bioorg. Med. Chem. Lett.*, 1993, **3**, 2471.

34 Y. Luo and G. D. Prestwich, *Bioconjugate Chem.*, 1999, **10**, 755.

35 A. Safavy, K. P. Raisch, M. B. Khazaeli, D. J. Bushsbaum and J. A. Bonner, *J. Med. Chem.*, 1999, **42**, 4919.

36 F. M. H. de Groot, W. A. Loos, R. Koekkoek, L. W. A. van Berkom, G. F. Busscher, A. E. Seelen, C. Albrecht, P. de Bruijn and H. W. Scheeren, *J. Org. Chem.*, 2001, **66**, 8815.

37 F. M. H. de Groot, L. W. A. van Berkom and H. W. Scheeren, *J. Med. Chem.*, 2000, **43**, 3093.

38 G. M. Dubowchik and S. Radia, *Tetrahedron Lett.*, 1997, **38**, 5257.

39 H. Sajiki, K. Hattori and K. Hirota, *J. Org. Chem.*, 1998, **63**, 7990.

Cancer Science
The official journal of the Japanese Cancer Association

NC-6300, an epirubicin-incorporating micelle, extends the antitumor effect and reduces the cardiotoxicity of epirubicin

Amane Takahashi,[1,2,3] Yoshiyuki Yamamoto,[1,4] Masahiro Yasunaga,[1] Yoshikatsu Koga,[1] Jun-ichiro Kuroda,[1] Misato Takigahira,[1] Mitsunori Harada,[5] Hiroyuki Saito,[5] Tatsuyuki Hayashi,[5] Yasuki Kato,[5] Taira Kinoshita,[2] Nobuhiro Ohkohchi,[3] Ichinosuke Hyodo[4] and Yasuhiro Matsumura[1,6]

[1]Division of Developmental Therapeutics, Research Center for Innovative Oncology, Kashiwa; [2]Upper Abdominal Surgical Oncology, National Cancer Center Hospital East, Kashiwa; [3]Department of Surgery, Advanced Biomedical Applications, University of Tsukuba, Tsukuba; [4]Department of Gastroenterology and Hepatology, Institute of Clinical Medicine, Graduate School of Comprehensive Human Sciences, University of Tsukuba, Tsukuba; [5]Research Division, NanoCarrier Co. Ltd., Kashiwa, Japan

(Received January 4, 2013/Revised February 25, 2013/Accepted March 11, 2013/Accepted manuscript online March 16, 2013/Article first published online April 19, 2013)

Epirubicin is widely used to treat various human tumors. However, it is difficult to achieve a sufficient antitumor effect because of dosage limitation to prevent cardiotoxicity. We hypothesized that epirubicin-incorporating micelle would reduce cardiotoxicity and improve the antitumor effect. NC-6300 comprises epirubicin covalently bound to PEG polyaspartate block copolymer through an acid–labile hydrazone bond. The conjugate forms a micellar structure of 40–80 nm in diameter in an aqueous milieu. NC-6300 (10, 15 mg/kg) and epirubicin (10 mg/kg) were given i.v. three times to mice bearing s.c. or liver xenograft of human hepatocellular carcinoma Hep3B cells. Cardiotoxicity was evaluated by echocardiography in C57BL/6 mice that were given NC-6300 (10 mg/kg) or epirubicin (10 mg/kg) in nine doses over 12 weeks. NC-6300 showed a significantly potent antitumor effect against Hep3B s.c. tumors compared with epirubicin. Moreover, NC-6300 also produced a significantly longer survival rate than epirubicin against the liver orthotopic tumor of Hep3B. With respect to cardiotoxicity, epirubicin-treated mice showed significant deteriorations in fractional shortening and ejection fraction. In contrast, cardiac functions of NC-6300 treated mice were no less well maintained than in control mice. This study warrants a clinical evaluation of NC-6300 in patients with hepatocellular carcinoma or other cancers. (*Cancer Sci* 2013; 104: 920–925)

Hepatocellular carcinoma (HCC) is the fifth most common cancer and the third largest cause of cancer mortality worldwide.[1,2] The range of available oncological treatment for HCC is sometimes limited due to poor liver function caused by concomitant chronic liver disease, especially liver cirrhosis, which is mainly the result of hepatitis virus infection. Surgical resection is widely considered the mainstay for curative treatment and yields a certain survival rate. However, <20% of patients with HCC can undergo surgical resection.[3,4] With the exception of patients at an early stage and with adequate liver function, recurrence rates after surgical resection are unfortunately high. High recurrence rates are also seen in patients treated by other local treatment options, such as ablation, percutaneous ethanol injection, and trans-arterial chemoembolization.[5] For advanced HCC, the only available option is sorafenib, a tyrosine kinase inhibitor, which was recently approved; however, the survival rate associated with its use is far from satisfactory.[6–8]

Anthracyclines such as epirubicin (EPI) and doxorubicin (DXR) are widely used and highly effective anticancer agents for the treatment of various human tumors including HCC, breast cancer, and gastric cancer.[9–13] However, anthracyclines induce several adverse effects, among which acute or chronic cardiotoxicity sometimes causes patients irreversible damage.[14–17] Cardiotoxicity of EPI is approximately 66% of that of DXR, but it is still the most serious problem in oncological treatment; this side-effect can sometimes require cessation of EPI treatment, resulting in an insufficient antitumor effect.[18–20] To address these issues, various anthracyclines have been developed to reduce cardiotoxicity without loss of the antitumor effect. However, to date, no such anthracyclines are available in a clinical context.

Against this background, NC-6300 was synthesized. NC-6300 comprises EPI covalently bound to PEG polyaspartate block copolymer through an acid–labile hydrazone bond. The conjugate spontaneously forms a micellar structure with a diameter of 40–80 nm in aqueous media, as reported previously.[21] *In vitro* findings indicated that it showed pH-dependent EPI release, namely, the release of EPI from NC-6300 accelerated under increasingly acidic conditions. NC-6300 is stable in the bloodstream for a long time; therefore, it accumulates selectively in tumor tissues through the enhanced permeability and retention effect.[21,22] Following the extravasation of NC-6300, NC-6300 or its disintegrated EPI-bound unimers reach and enter cancer cells. Then, under the acidic conditions within lysosomes, EPI may be released, leading to the subsequent death of the cancer cells.

In this study, we evaluated the antitumor effect of NC-6300 using mouse models with human HCC Hep3B cells. Moreover, we examined the cardiotoxicity of NC-6300, particularly in terms of cardiac function, by using echocardiography over a long period.

Materials and Methods

Drugs. NC-6300 was supplied and synthesized by NanoCarrier (Kashiwa, Japan) (Fig. 1). The synthesis was described elsewhere.[21] NC-6300 was stored in a frozen state at −80°C and melted on ice immediately before inoculation into mice. Then, the NC-6300 was prepared with distilled water at 1.0 mg/mL (epirubicin-equivalent dose). NC-6300 is stable at low temperatures under neutral conditions, but gradually begins to release the encapsulated EPI in an acidic environment.[21] The EPI was purchased from Pfizer Japan (Tokyo, Japan).

Cell culture. The human HCC cell line Hep3B was obtained from the European Collection of Cell Culture (ECACC, Salis-

[6]To whom correspondence should be addressed.
E-mail: yhmatsum@east.ncc.go.jp

doi: 10.1111/cas.12153

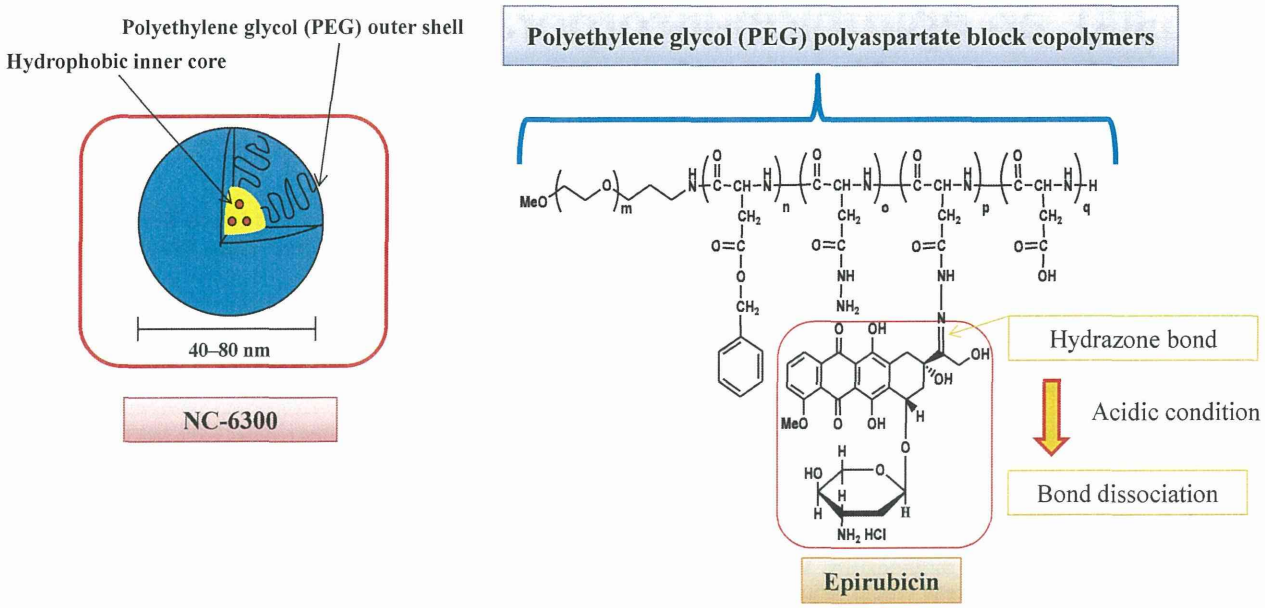

Fig. 1. NC-6300 comprises epirubicin covalently bound to the polyaspartate chain of PEG polyaspartate block copolymer by an acid–labile hydrazone bond. The conjugate spontaneously forms a micellar structure in an aqueous milieu. The diameter of NC-6300 is 40–80 nm, and the micellar formulation is stable under physiological conditions.

bury, UK). Hep3B cells were cultured in DMEM supplemented with 10% FBS (Cell Culture Technologies, Gaggenau-Hoerden, Germany), penicillin, streptomycin, and amphotericin B (100 units/mL, 100 μg/mL, and 25 μg/mL, respectively; Sigma, St. Louis, MO, USA) in humidified 5% CO_2 at 37°C.

Establishment of Hep3B cell line stably expressing firefly luciferase. For the *in vivo* bioluminescence imaging of liver orthotopic tumors, the Hep3B cell line stably expressing firefly luciferase (Hep3B/Luc) was established. Briefly, the coding sequence for firefly luciferase was subcloned into the pcDNA3.1(+) vector (Invitrogen, Carlsbad, CA, USA) to generate plasmids of pcDNA3.1/luciferase. Hep3B cells (2×10^5) were seeded onto 3-cm dishes 24 h before transfection. The cells were transfected with 2.5 μg plasmid DNA using Lipofectamine LTX Reagent and PLUS Reagent (Invitrogen) in accordance with the manufacturer's instructions, then incubated for 48 h at 37°C. The cells were then passaged in medium containing G418 (1 mg/mL; Invitrogen) to select for the neomycin-resistance gene integrated in the pcDNA3.1(+) plasmids. The accuracy of a quantitative bioluminescence image as an indicator of Hep3B/Luc cell number was analyzed using the IVIS Kinetic Imaging system (Caliper Life Sciences, Hopkinton, MA, USA) *in vitro*, as described below. This analysis showed a clear correlation between a quantitative bioluminescence image and cell number. The sensitivity of Hep3B/Luc cells to each anticancer drug was similar to that of parental Hep3B cells (data not shown).

Orthotopic tumor model. Six- to eight-week-old female BALB/c nude mice (CLEA Japan, Tokyo, Japan) each weighing approximately 20 g at the time of surgery were used for *in vivo* studies. The animals were maintained under specific pathogen-free conditions in cages, provided with standard food, and given free access to sterilized water. All animal procedures were carried out in compliance with the Guidelines for the Care and Use of Experimental Animals established by the Committee for Animal Experimentation of the National Cancer Center, Japan; these guidelines meet the ethical standards required by law and also comply with the guidelines for the use of experimental animals in Japan.

The HCC model was created by direct intrahepatic inoculation of Hep3B/Luc cells. The mice were anesthetized by i.p. injection of 0.15 mL/g body weight of 2,2,2-tribromoethanol in 2-methyl-2-butanol. The stock solution of the anesthetic is 1.0 g 2,2,2-tribromoethanol (Wako, Osaka, Japan) dissolved in 1.0 mL 2-methyl-2-butanol (Sigma). Just before use, 1 mL stock solution was diluted with 40 mL H_2O. A short median laparotomy was carried out with disinfection of the abdominal skin. Then, 5×10^6 Hep3B/Luc cells suspended in 20 μL Matrigel (BD Biosciences, San Jose, CA, USA) were directly injected into the left lower lobe of the liver using a 29-gauge needle. To prevent either bleeding or dissemination of tumor cells, puncture sites were ablated with a bipolar cautery.

***In vivo* tumor growth inhibition assay.** *Experiment 1.* Six-week-old BALB/c nude mice (CLEA Japan) were s.c. inoculated with 1×10^7 Hep3B/Luc cells in the flank region. When the tumor volume reached 150 mm^3, the mice were randomly divided into test groups consisting of six mice per group (day 0). Drug was given i.v. on days 0, 7, and 14 through the lateral tail vein. NC-6300 was given at 10 and 15 mg/kg and the reference drug, EPI, was given at its maximum tolerated dose of 10 mg/kg. The length (a) and width (b) of s.c. tumors and body weight were measured twice a week, and tumor volume (TV) was calculated as follows: $TV = (a \times b^2)/2$. Relative body weight (RBW) on day n was calculated according to the following formula: $RBW = BW_n/BW_0$, where BW_n is the body weight on day n and BW_0 is the body weight on day 0.

Experiment 2. Two weeks after direct hepatic inoculation of Hep3B/Luc cells, mice were randomly divided into three tests groups consisting of 10 mice per group (day 0). Randomization was carried out on the basis of bioluminescence images, and we confirmed that the mean values of count per minute in the images were not significantly different between groups. The mice were given i.v. injections into the lateral tail vein (200 μL) at 10 mg/kg or 15 mg/kg NC-6300, or 10 mg/kg

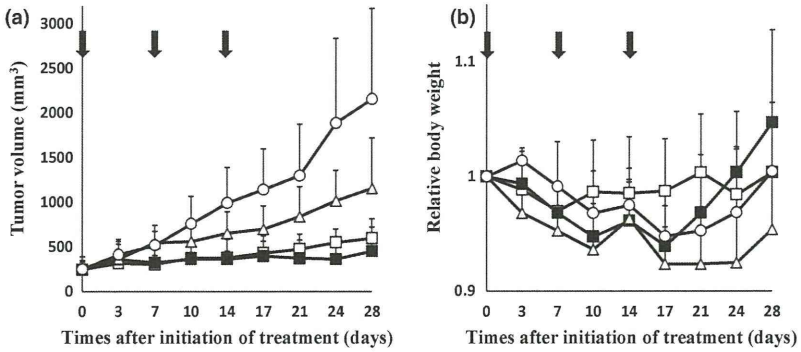

Fig. 2. Antitumor effects of NC-6300 and epirubicin (EPI) in mice bearing s.c. Hep3B xenografts. Hep3B cells (1×10^7 cells) were inoculated s.c. on the back. NC-6300 or conventional EPI was injected i.v. on days 0, 7, and 14. Day 0 indicates the day when tumor volume reached 150 mm^3 ($n = 6$). The dose of NC-6300 is expressed as dose equivalent of EPI. ○, Control; □, NC-6300 at 10 mg/kg; ■, NC-6300 at 15 mg/kg; △, EPI at 10 mg/kg. (a) Antitumor activity of NC-6300 or EPI was evaluated by measuring the tumor volume. The ANOVA test between NC-6300 (10 mg/kg) and EPI (10 mg/kg), $P = 0.0017$; NC-6300 (15 mg/kg) and EPI (10 mg/kg), $P < 0.001$. (b) Changes in relative body weight. Data were derived from the same mice as those used in the treatment experiment. The ANOVA test between NC-6300 (10 mg/kg) and EPI (10 mg/kg), $P = 0.0053$; NC-6300 (15 mg/kg) and EPI (10 mg/kg), $P < 0.001$. Arrows, drug injections; bars, SD; points, mean.

EPI, on days 0, 7, and 14. Control mice were injected with 200 μL PBS following the same schedule. To evaluate the progression of orthotopic liver tumor, *in vivo* bioluminescence imaging was carried out with the IVIS Kinetic Imaging system (Caliper Life Sciences) every week from the day of treatment initiation, and the body weight of each mouse was also measured. Mortality and morbidity were checked daily and the mice were maintained until each one showed signs of morbidity (massive ascites or hepatic tumor that could be observed through skin, jaundice, and 20% weight loss), at which point they were killed.

Pharmacokinetics of EPI and NC-6300 in mice. Four weeks after direct tumor inoculation of Hep3B/Luc in the liver, either EPI (10 mg/kg) or NC-6300 (10 mg/kg) was injected i.v. Before sampling, the mice were anesthetized with ether. Plasma, tumor, liver, heart, kidney, spleen, and lung were obtained and weighed at 1, 6, 12, 24, and 72 h. Tissue samples were rinsed with saline and stored at −80°C until use.

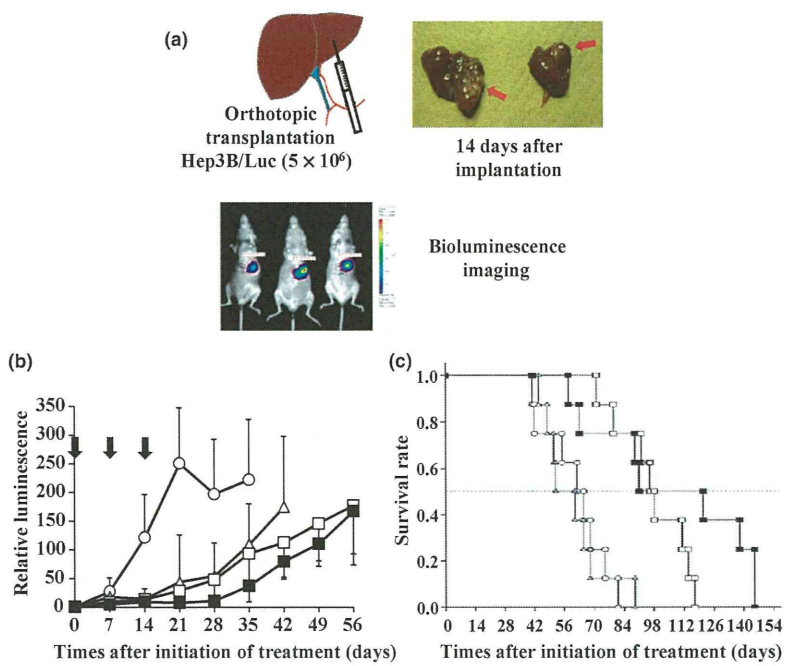

Fig. 3. (a) Orthotopic liver tumor xenografts and evaluation of tumor growth using bioluminescence imaging. Hep3B/Luc cells (5×10^6) suspended in 20 μL Matrigel were directly injected into the left lower lobe of the liver in mice using a 29-gauge needle. To visualize and evaluate the transplanted hepatic tumor of Hep3B/Luc cells, *in vivo* bioluminescence imaging was carried out. (b) Antitumor effect of NC-6300 and epirubicin (EPI) in mice bearing Hep3B/Luc xenografts. Each drug was given on days 0, 7, and 14 after tumor implantation ($n = 8$). The antitumor activity was evaluated by determining the relative photon count. The ANOVA test between NC-6300 (15 mg/kg) and EPI (10 mg/kg), $P = 0.025$. Arrows, drug injections; bars, SD; points, mean. (c) Kaplan–Meier curves. Log–rank test, NC-6300 (10 mg/kg) group *versus* EPI (10 mg/kg) group, $P = 0.002$; NC-6300 (15 mg/kg) group *versus* EPI (10 mg/kg) group, $P = 0.004$. ○, Control; □, NC-6300 at 10 mg/kg; ■, NC-6300 at 15 mg/kg; △, EPI at 10 mg/kg.

doi: 10.1111/cas.12153

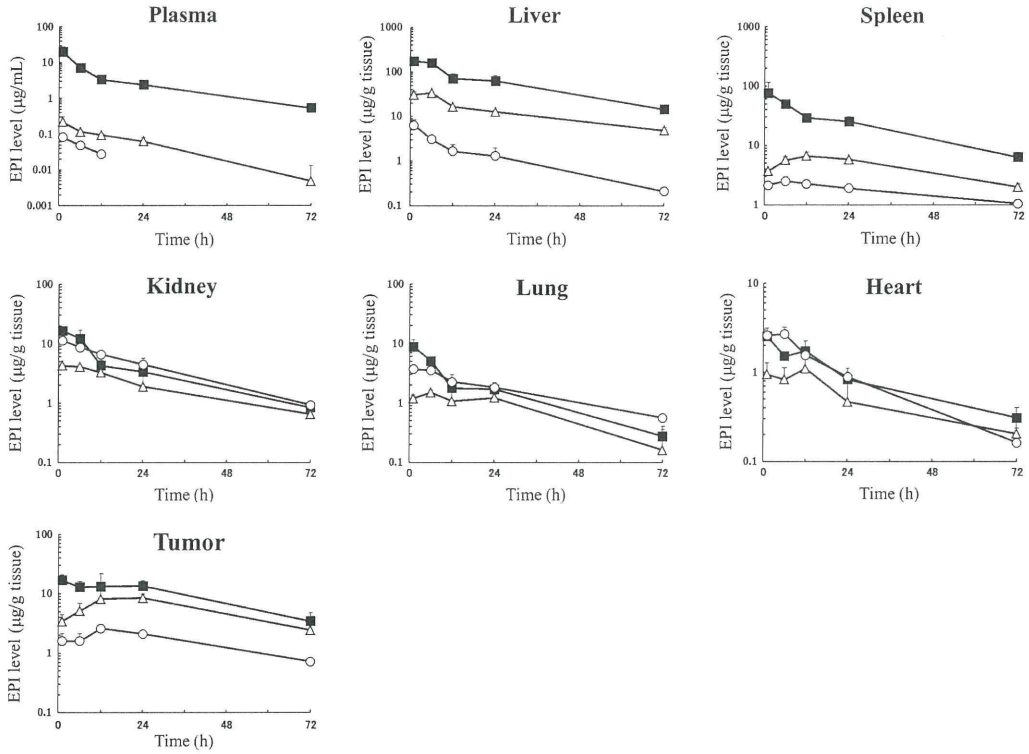

Fig. 4. Plasma and tissue concentration–time profiles of total (■) and released (Δ) epirubicin (EPI) after i.v. injection of NC-6300 (10 mg/kg) into mice bearing Hep3B/Luc orthotopic liver tumors. Plasma and tissue concentration–time profiles of EPI after conventional EPI (10 mg/kg) (○) injection. Data points are the means of three mice.

Table 1. Area under the time–concentration curve (AUC) values in plasma and tissues after injection of NC-6300 at 10 mg/kg or epirubicin (EPI) at 10 mg/kg in mice bearing orthotopic Hep3B/Luc liver xenografts

	AUC (μg/g tissue or mL × h)				
	NC-6300			Conventional EPI	Released/Conventional EPI AUC ratio
	Released EPI	Total EPI	% Released		
Plasma	4.1	213.0	1.9	0.6	6.95
Liver	920.5	4246.8	21.7	94.9	9.70
Spleen	323.3	1657.3	19.5	121.9	2.65
Kidney	136.2	273.5	49.8	295.2	0.46
Lung	61.4	127.2	48.3	118.7	0.52
Heart	36.2	63.7	56.9	66.9	0.54
Tumor	422.5	724.2	58.3	116.8	3.62

Tissue samples were suspended in 0.1 M sodium phosphate buffer (pH 7.4) at a concentration of 25% w/w and homogenized on ice using Precellys 24 (Bertin Technologies, Montigny-le-Bretonneux, France). Using aliquots of the homogenates and plasma (50 μL), concentrations of the EPI released from NC-6300 *in vivo* and the total EPI (free EPI released from NC-6300 *in vivo* and the polymer-bound EPI) were determined.

To determine the concentration of released EPI, the homogenates and plasma samples (50 μL) were treated with acetonitrile (125 μL) to precipitate proteins. Then, 1% Triton X-100 (25 μL) was added and the sample was vortexed and centrifuged for 5 min at 5000 *g* at 4°C. Subsequently, 75 μL daunorubicin HCL (2 μg/mL)/20 mM sodium phosphate buffer (pH 7.4) was added to the supernatant (75 μL) as an internal control. The prepared mixture was analyzed by HPLC. To determine the total EPI concentration, the samples (50 μL) were treated with acetonitrile (130 μL) and acidified with 1 N HCL (20 μL) for 1 h at room temperature to allow the complete release of EPI from NC-6300. Next, 1% Triton X-100 (25 μL) was added and the sample was vortexed and centrifuged for 5 min at 5000 *g* at 4°C. Then, 75 μL daunorubicin HCL (2 μg/mL)/25 mM ammonium formate buffer (pH 3.0) was added to the supernatant (75 μL) as an internal control. The prepared mixture was analyzed by HPLC.

Reversed-phase HPLC was carried out at 40°C on a Tosoh TSK-gel ODS-80Tm (4.6 ϕ × 150 mm; Tosoh, Tokyo, Japan) with a Tosoh ODS-80Tm guard cartridge. The EPI was eluted with 25 mM ammonium formate buffer (pH 3.0):acetonitrile (70:30, v/v) using a Waters Alliance System (Waters Corporation, Milford, MA, USA) at a flow rate of 1.0 mL/min. Detec-

tion was carried out using a Waters fluorescence detector with excitation and emission wavelengths of 488 and 560 nm, respectively.

Echocardiography for mice. To investigate the acute and chronic cardiotoxicity induced by EPI, we designed the following experimental scheme. Five-week-old female C57BL/6 mice were given NC-6300 at a dose of 10 mg/kg or EPI at 10 mg/kg (n = 6) on days 0, 7, and 14, and the mice were left for an interval of 7 days. We repeated this schedule three times; namely, mice were given each drug nine times in total. We evaluated the cardiac function using echocardiography on days 0, 7, 14, 21, 49, and 77.

Echocardiography was carried out using a high-resolution Micro Ultrasound system (Vevo 770; VisualSonics, Toronto, Canada), equipped with a 40-MHz ultrasound probe (RMV704; VisualSonics). Mice were kept under light sedation with 1–2% isoflurane until the heart rate stabilized at between 400 and 500 beats per minute. Left ventricular dimensions and wall thicknesses were determined from parasternal short-axis M-mode echocardiography images, and fractional shortening (FS) and ejection fraction (EF) were automatically calculated with Vevo 770 software.

Statistical analysis. Data are expressed as the mean ± SD. To evaluate antitumor effects, changes in body weight, and changes in cardiac function, repeated-measures ANOVA was carried out using StatView 5.0 software (Statview, Hulinks, Tokyo, Japan). Survival was assessed by the Kaplan–Meier method using SPSS version 19 software (SPSS Inc., Chicago, IL, USA). For all tests, P-values <0.05 were considered to be statistically significant. All statistical tests were two-sided.

Results

Antitumor activity of NC-6300 and epirubicin in mice bearing Hep3B s.c. tumor. NC-6300 given at 10 or 15 mg/kg three times with a 7-day interval appeared to possess significantly superior antitumor activity compared with EPI given at 10 mg/kg with the same schedule. The group treated with EPI at 10 mg/kg showed a significant decrease in body weight as compared with the groups treated with NC-6300 at 10 and 15 mg/kg (Fig. 2).

Antitumor activity of NC-6300 and epirubicin in mice bearing Hep3B/Luc liver orthotopic tumors. Antitumor activity was observed in mice bearing Hep3B/Luc xenografts implanted orthotopically following treatment with NC-6300 at 10 or 15 mg/kg or EPI at 10 mg/kg (Fig. 3). There was a significant difference between the control group and the groups treated with EPI and NC-6300 (Fig. 3b). Comparison of the relative photon count revealed significant differences between NC-6300 at 15 mg/kg and EPI at 10 mg/kg (Fig. 3b). Kaplan–Meier analysis showed that there was a significant improvement in the survival rate in the group given NC-6300 at 10 mg/kg compared with that in the group given EPI at 10 mg/kg (P = 0.002), as well as for the group given NC-6300 at 15 mg/kg compared with the group given EPI at 10 mg/kg (P = 0.004) (Fig. 3c).

Tissue distribution of NC-6300 and epirubicin in mice bearing orthotopic Hep3B/Luc tumor. Tissue distribution experiments were carried out to evaluate the toxicity and efficacy data obtained for both NC-6300 and EPI in terms of the plasma and tissue concentrations of each formulation. The concentration–time profiles in plasma and various tissues were obtained (Fig. 4) and the results were similar to previous data.[21] After the injection of EPI, its concentration declined rapidly. On the other hand, NC-6300 showed significantly slower clearance. The clearance rate of NC-6300 in orthotopic Hep3B tumors was significantly slower than that of other normal organs. In a similar manner to other drugs categorized in the drug delivery system, NC-6300 showed higher accumulation in organs of the reticuloendothelial system. In heart, a significantly higher concentration of EPI was obtained for several hours after treatment with conventional EPI compared with that of NC-6300. To compare the tissue accumulation of EPI released from NC-6300 with that of EPI after treatment with conventional EPI, the area under the time–concentration curve (AUC) values in each tissue were determined, as summarized in Table 1. NC-6300 produced increases in EPI concentration, particularly in the plasma, liver, spleen, and tumor, whereas NC-6300 decreased the free EPI concentration in kidney, lung, and heart.

Echocardiogram following treatment of NC-6300 and epirubicin. Cardiotoxicity was evaluated by echocardiography in C57BL/6 mice during and following a total of nine treatments with NC-6300 (10 mg/kg) and conventional EPI (10 mg/kg) over 12 weeks. The EF of mice treated with conventional EPI (10 mg/kg) was significantly reduced compared with those of the control (P = 0.0019) and NC-6300 (10 mg/kg) treatment groups

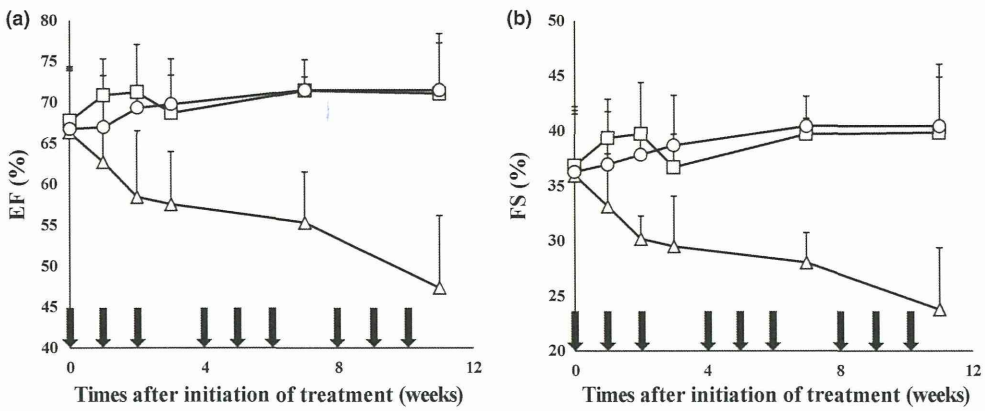

Fig. 5. Echocardiography for evaluating cardiotoxicity. C57BL/6 mice were given NC-6300 (10 mg/kg) or conventional epirubicin (EPI; 10 mg/kg) on days 0, 7, and 14 every 4 weeks, for a total of nine injections of each drug over 12 weeks (n = 6). ○, Control; □, NC-6300 at 10 mg/kg; △, EPI at 10 mg/kg. Left ventricular dimensions and wall thicknesses were determined from the echocardiography images, and ejection fraction (EF) and fractional shortening (FS) were automatically calculated. (a) Changes in EF; ANOVA test between NC-6300 (10 mg/kg) and EPI (10 mg/kg), P = 0.0081. (b) Changes in FS; ANOVA test between NC-6300 (10 mg/kg) and EPI (10 mg/kg), P = 0.0114. Arrows, drug injections; bars, SD; points, mean.

doi: 10.1111/cas.12153